SEISMIC WAVE PROPAGATION CHARACTERISTICS USING CONVENTIONAL AND ADVANCE MODELLING ALGORITHM FOR D-DATA IMAGING

[1] *School of Physics, Geophysics Section, Universiti Sains Malaysia, USM, Penang, Malaysia. Yasir.bashir@usm.my*
[2] *Centre for Seismic Imaging, Geosciences Department, Universiti Teknologi Petronas, Malaysia.*
[3] *Institute of Geophysics, Polish Academy of Sciences, Warsaw, Poland*
[4] *Department of Earth Sciences, University of Sargodha, Sargodha, Pakistan*
[5] *Center of Petroleum Studies, University of Campinas, Campinas, Sao Paulo, Brazil.*

Bashir, Y., Babasafari, A.B., Alashloo, S.Y.M., Muztaza, N.M., Ali, S.H. and Imran, Q.S., 2020. Seismic wave propagation characteristics using conventional and advance modelling algorithm for D-data imaging. *Journal of Seismic Exploration*, 30: 21-44.

The importance of seismic imaging is being impetrative in the petroleum industry because of exploiting minor hydrocarbon reservoirs traps in highly tectonic and complex structures increased. The primary objective of diffraction data imaging is to improve the image of subsurface in looking for structural topographies and the extreme super resolution which can express the sharpness and insides feature in it. These high-resolution images are tools for interpreters to allow for immediate proof of identity the smaller events, pitchouts and edges of the anomalies such as faults, fractures and Salt bodies. After the seismic imaging technology is being advance in recognition of the diffracted wave which is found is a carrier of the high-resolution imaging. In this paper, an algorithm is introduced based on low-rank symbol approximation for modelling the seismic wave propagation. The results demonstrate a dispersion free modelled data which is further used for D-data (diffraction data) imaging. The modelling is performed using low-rank (LR) and Finite difference (FD) methods and observed LR is better than FD. The results of the D-Data images show an enhancement in the band of frequency from 0 to 10 Hz and from 50 to 60 Hz. This paper demonstrates how this can be used to assess the characteristics of subsurface features and enhance the resolution of seismic data to explore the hydrocarbon reservoir.

KEY WORDS: finite difference, low-rank, wave modelling, diffraction, high-resolution.

0963-0651/21/$5.00

INTRODUCTION

It is difficult to read a road symbol if a person has a weak vision, therefore a driving license is issued with the limitations requiring that corrective lenses must be worn. Similarly, it is tough to explore subsurface reserves if a geoscientist cannot clearly see the target or monitor the movement of fluids in the subsurface reservoir (Neal and Krohn, 2012). The oil & gas exploration company's goal is to constantly improve the subsurface seismic data to find and produce oil & gas in the reservoirs. Seismological research that addresses the imaging limitation is advancing worldwide on acquiring data with a new array of technologies but the problems such as layers of salt, thrust sheets, fractured basement, Carbonate Karstification, gas masking effect, and unknown medium highlight not only the challenges to achieving higher resolution, but also concern on depth conversion.

Seismic wave propagation in time plays a substantial role in seismic modelling and depth imaging. Currently, in the conventional way of wave extrapolation method is implemented by Finite Difference Modelling (FDM) (Etgen and Brandsberg-Dahl, 2009). Theoretically speaking, high-resolution seismic diffraction images enable one to image details outside the classical Rayleigh boundary of half a seismic wavelength. Diffracted waves have thoroughly examined in the seismic literature because of their imaginary and practical importance in modelling, imaging, and interpretation (Coimbra et al., 2018). Improvements in high-resolution imaging methods through diffraction are already explained in many published papers, for example Bansal and Imhof, 2005; Fomel et al., 2007; Landa and Keydar, 1998; Taner et al., 2006.

The systematic technique comprises the designing of wave extrapolation operatives by reminiscent of the space wavenumber matrix symbol with a low-rank decomposition. The method used in this paper involved selecting a small set of representative spatial locations and a small set of representative wavenumbers. Nevertheless, the LR algorithm implementation is more expensive than FD in the sense of computational power and time consumption but the results accuracy is higher. LR algorithm was extended to anisotropic media for wave propagation back in 2009 by Behura and Tsvankin, in 2013 by Fomel et al., and then by Bashir et al. (2016, 2017, 2018, 2019, 2020). They involve the Eigenfunction instead of the columns and rows of the original extrapolation matrix (Song et al., 2013).

It is normal practice to use a second order Finite Difference for temporal derivatives and high-order Finite Difference for spatial derivatives, to reduce the noise and the dispersion for improving the accuracy of the output data. The coefficients of the Finite Difference methods are calculated using a Taylor series expansion around zero wavenumbers (Dablain, 1986; Kindelan et al., 1990). Improvements in the FD method has applied previously, for example one-way wave extrapolation. Holberg (1987, 1988)

has improved the FD method by matching the spectral response in the wavenumber domain. The FD method has been further developed by researchers over the last decade (Liu and Sen 2011; 2009; Mousa et al. 2009; Soubaras 1996; Takeuchi and Geller 2000; Holberg 1988; Holloway 1981) but the method is still slightly poor when trying to model seismic data without noise and dispersion.

The technique of "D-Data imaging" used in this paper entails the separation of the diffraction data through the well-known Claerbout method of "plane-wave destruction" (PWD). The proposed method is opposite to the more common "full-wave imaging", which images a full shot record of all the information including reflection, diffractions, and multiples.

This paper inspects the challenges of getting a high-resolution of subsurface structural images in case of complex Salt deposit which leads to the emerging research trends for strong reflection and diffraction imaging technologies aimed at carrying a more precise reservoir. We first introduce the wave modelling method (the low-rank approximation method) which provides an accurate wave extrapolation method. Next, the paper presents wave modelling using the FD method in a smooth velocity model which is then compared with the LR method to give improved and dispersion-free results. Furthermore, this approach is applied to the Sigsbee model in order to compare diffraction migration and full wave migration. The Marmousi data set is then used to enhance the resolution of the seismic data through diffraction and reflection imaging, separately. A frequency spectrum of both datasets demonstrates that diffraction imaging can enlarge the bandwidth of the data at low frequencies (0 - 10 Hz) and higher frequencies (40 - 60 Hz).

Theory & Method for Advance Wave Modelling

Here, we present the theory behind the algorithm and tested its correctness on artificial data from the Gulf of Mexico. The wave equation is a linear second-order partial differential equation which describes the propagation of oscillations at a fixed speed in some quantity of

$$\frac{1}{v^2}\frac{\partial^2 y}{\partial t^2} = \frac{\partial^2 y}{\partial x^2} \quad , \tag{1}$$

where v is the velocity of wave, and t is traveltime of the wave propagation. Plane wave in physical model, we can define the mathematically as,

$$\frac{\partial P}{\partial x} + \sigma \frac{\partial P}{\partial t} = 0 \quad , \tag{2}$$

where ∂P is the wave field and σ is the local slope which is dependent on distance (x) and traveltime (t).

In eq. (3), *P(x,t)* is wavefield of seismic at spatial position x and temporal time t . Wavefield on the subsequent time step (*t*+*dt*) is estimated using given operator below (Wards et al., 2008).

$$P(x, t + \Delta t) = \int \hat{P}(k, t) e^{i \emptyset(x,\ k,\ \Delta t)} dK \quad , \tag{3}$$

here $\hat{P}(k, t)$ is an spatial Fourier transform of $P(x, t)$ and

$$\hat{P}(k, t) = \frac{1}{2\pi^3} \int P(x, t) e^{-i\, kx}\, dx \quad , \tag{4}$$

where k represents the wavenumber in the spatial domain. $\emptyset(\mathrm{x}, \mathrm{k}, \Delta\mathrm{t})$ describes the function of phase that seems in eq. (3), which can be rough calculate into the equation of wave and then extract geometrical higher frequency asymptotic of its. Eikonal-like equation is led in the case of seismic wave propagation (Fomel et al., 2013):

$$\frac{\partial \emptyset}{\partial t} = \pm V(x, k) \ \ |\nabla \emptyset| \quad , \tag{5}$$

where $V(x, k)$ is the velocity of phase function, If we assume small incremental phases Δt in eq. (3), this can be used to shape successive guesstimates for phase function $\emptyset$ by intensifying it into a Taylor series (TS). In individual, the presentation of the phase function is given below:

$$\emptyset(x, k, t) \approx k \,.x + \emptyset_1(x, k)t + \emptyset_2(x, k)\frac{t^2}{2} + \cdots \quad . \tag{6}$$

Respectively,

$$|\nabla \emptyset| \approx |k| + \frac{\nabla \emptyset_1 . k}{|k|} t + O(t^2) \quad . \tag{7}$$

Replacing eqs. (6) and (7) in eq. (5) and unraveling the terms with dissimilar powers of t, we found:

$$\emptyset_1(x, k) = V(x, k)|k| \quad , \tag{8}$$

$$\emptyset_2(x, k) = V(x, k) \nabla V . k \quad . \tag{9}$$

In the case of gradient velocity ∇V and the time step ∇*t* is small, then the Taylor expansion of eq. (7) will be condensed to double terms, in the sense, decreases eq. (3) to an aware appearance (Etgen and Brandsberg-Dahl, 2009).

$$P(x, t + \Delta t) \approx \int \hat{P}(k, t)\, e^{i[kx + V(x,k)|k|\Delta t]} dk \ , \qquad (10)$$

or

$$P(x, t + \Delta t) + P(x, t - \Delta t) \approx 2 \int \hat{P}\,(k, t) e^{ikx} \quad \cos[V(k, t)|k|\Delta t]\, d\mathrm{k} \quad (11)$$

In the case of the velocity model (which is rough and the ∇V gradient does not exist), eq. (5) can be solved numerically or by applying approximations instead of the Taylor expansion (6).

Low-rank Approximation

Actually, the low-rank estimation is a reducing function problem in which the total function measures the best fit between some given matrix data and approximating matrix data. All these processes lead to the constraint that the approximating matrix has a reduced rank up to the optimum rank. The main idea behind low-rank decomposition is to decompose the wave extrapolation matrix, thus:

$$W(x, k) = \ e^{i[\emptyset(x,k,\Delta t) - kx]} \qquad . \qquad (12)$$

Here $W(x, k)$ is the Acoustic wave field for a fixed Δt, a separated representation could be:

$$W(x, k) \approx \sum_{m=1}^{M} \sum_{n=1}^{N} W(x, k_m) a_{mn} W(x_n, k) \qquad . \qquad (13)$$

Representation (13) fasting the computation as the P $(x, t, \Delta t)$ are defined in eq. (14) which simply optimize the calculation up to the optimum rank, since:

$$P(x, t + \Delta t) = \int e^{ixk}\, W(x, k) \hat{P}(k, t) dk$$

$$\approx \sum_{m=1}^{M} W(x, k_m) \left(\sum_{n=1}^{N} a_{mn} \left(\int e^{ixk}\, W(x_n, k) \hat{P}\,(k, t) dk \right) \right) \qquad . \qquad (14)$$

$P(x, t + \Delta t)$ is wave field of the P-wave at a distance x and time t and $\hat{P}$ is the 3D Fourier transform of P**.** The expression of eq. (14) is effectually equivalent to put on N inverse to the Fast Fourier Transform. Numerically, a distinguishable low-rank approximation amounts to choosing a set of representative a wavenumber (M) and spatial locations (N) (Bashir et al., 2016a).

Diffraction vs. Reflection

Diffraction is a fundamental concept in light or wave propagation, and it constitutes the heart of an imaging process. As Fig. 1 shows the light source which is passing through a slit, supposedly the other side should be light and dark portion but because of slit's edges (known as Huygen's sources) produce a diffracted light which is slightly darker in nature. This same principle executes in the seismic wave propagation shown in Fig. 2. The source and receiver's geometry on the surface for recording a discontinuous layer in the subsurface. The "Off reflector" means the acquisition geometry is above no reflection and "On reflector" means the source and receiver are above the reflector. The recorded data shows seismic reflection on the continues and the edges of the horizon a diffraction hyperbola is produced. The + and – signs show the polarity of the amplitude recorded either side of the hyperbola (Berryhill, 1977; Hilterman, 1970, 1975). More elaboration of these seismic diffraction events is recognized by opposite in polarity on either side of the hyperbola as shown in Fig. 3(a). Once these negative and positive amplitudes cancel out, the only one dominant trace is left behind which represents the reflection [Fig. 3(b)].

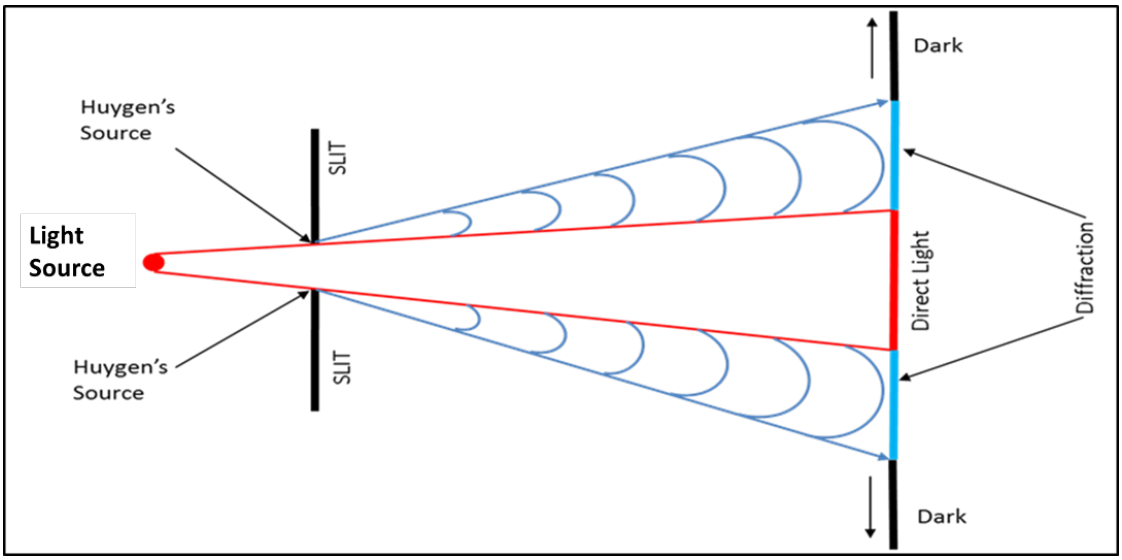

Fig. 1. Diffraction theory in a light wave, passing through a Slit causing a diffracted light. Source of diffraction is the edges of Slit as Huygen's sources.

Better Amplitude & Phase Preservation

Reflection seismology does not explain the seismic amplitude and phase but diffraction seismology explains these seismic parameters accurately. There is an 180^0 change in phase from positive to negative on either side of the hyperbola as shown in Fig. 3. Based on diffraction seismology each reflection point is produced after the cancelation of diffraction energy on both sides of the flank which preserve proper amplitude of the seismic wave.

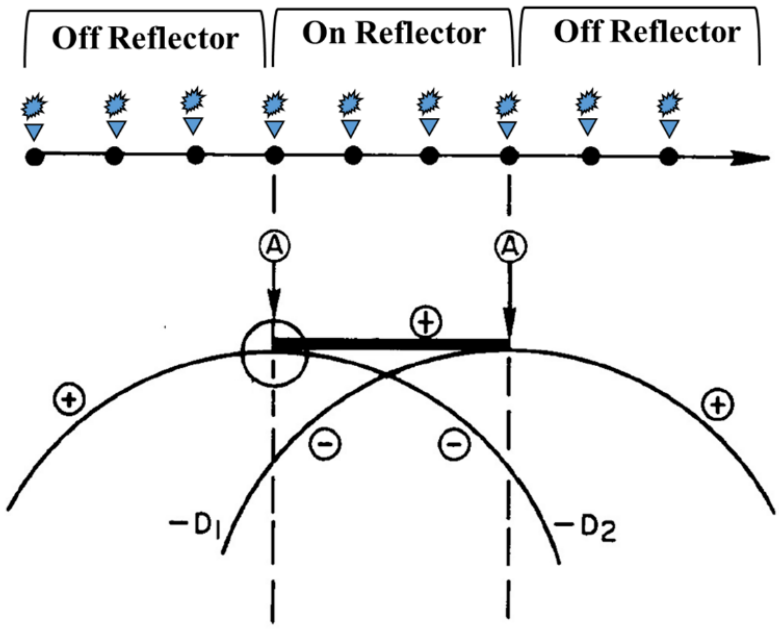

Fig. 2. Acquisition geometry for a discontinuous layer. Diffraction hyperbola is produced on the edges of the layer.

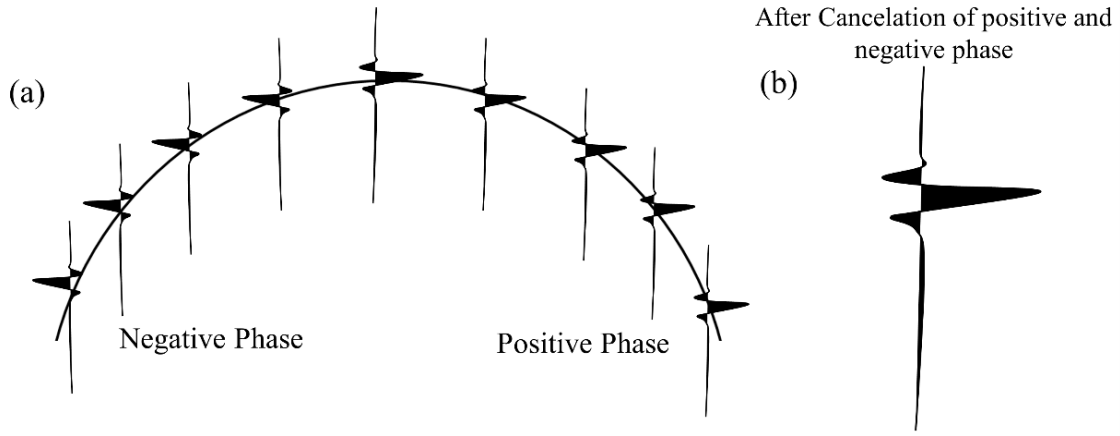

Fig. 3. (a) Illustration of diffraction hyperbola in 2D common-offset section in which positive and negative phase change of 180^0, and (b) After summation of the diffraction the concentrated energy in the apex only one trace left behind to produce a reflection.

Seismic Wave Modelling

Wave modelling is conducted through different approaches: Finite Difference (Fig. 4a) and low-rank approximation (Fig. 4b). The velocity of the model in this example is a smooth and the source with input ricker wavelet, which is placed at the center of the model. FDM results show the dispersion artifacts whereas, the outcome of the low-rank approximation corresponding to that of the Fourier Finite Difference (FFD) method, is dispersion-free, as shown in Fig. 4b with a better reflection, easily interpretation and no noise artifacts. Further, the amplitude spectrum of the two methods are plotted in Fig. 5, that shows a clear identification of signal

using low-rank can be achieved in the other hand finite difference modeling algorithm provide data with noise.

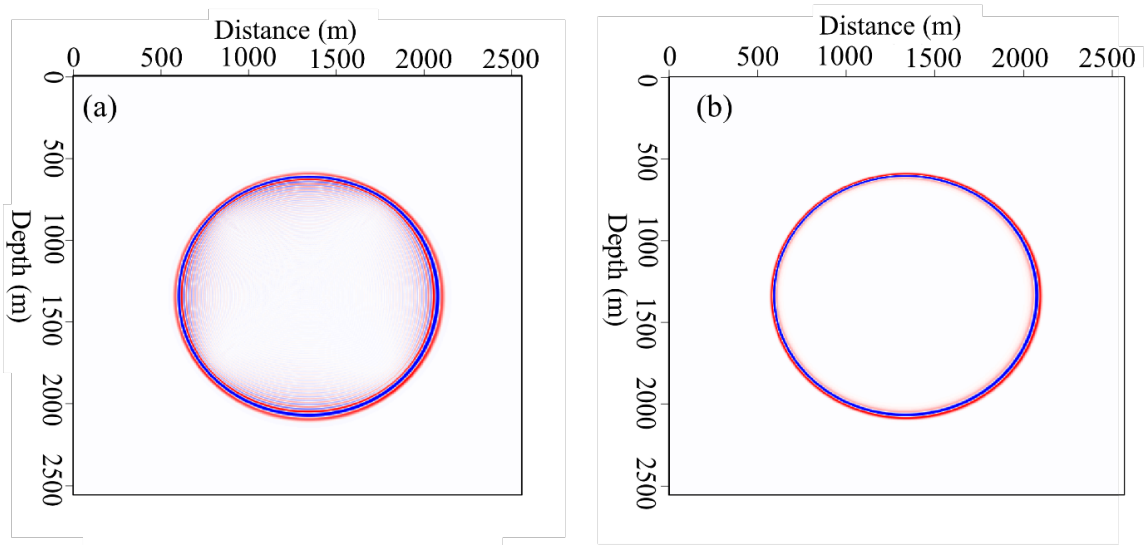

Fig. 4. (a) Captured Snap of a wavefield propagation in the velocity model computed using the FD modelling, and (b) The LR wavefield in the same velocity model.

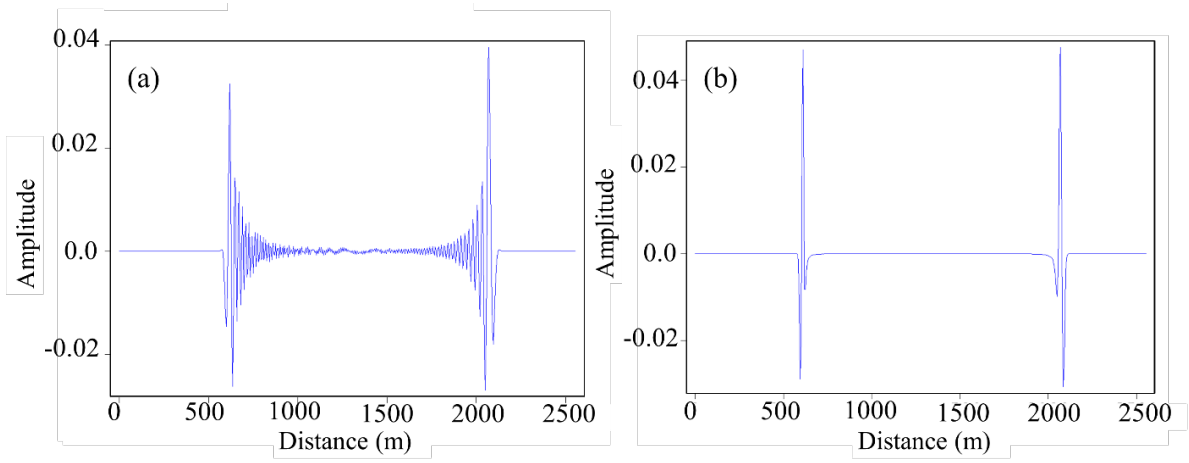

Fig. 5. Amplitude display of the propagated wavefield in 2-layer velocity model using (a) Finite Difference method, and (b) Low-rank modeling method.

The workflow used in this research study is shown in Fig. 6. It starts with the velocity model, which is converted into a reflectivity series for modelling. The reflectivity is achieved by the acoustic impedance contrast of velocity and density. After that zero-offset data is acquired by FD and LR modelling algorithm, full-wave migration, and diffraction migration is applied to the data. The payback of the diffraction migration is to identify important small-scale events, which could not be counted in the normal reflection imaging.

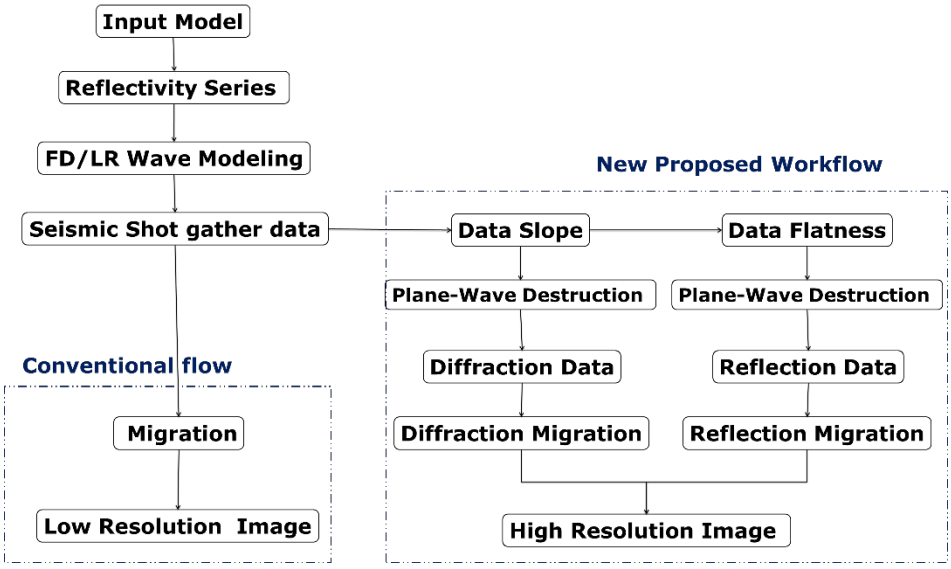

Fig. 6. Conventional and proposed workflow diagram for high-resolution imaging.

RESULTS and DISCUSSIONS

Examples of a Salt deposit model from GOM: The Sigsbee

Most of the subsurface information obtained from super-resolution seismic images are the result of diffraction consideration in imaging. The concern of these diffractions is necessary during advanced processing because, in conventional processing, diffraction data is removed either intentionally or implicitly. Separation of these diffractions before filtering is necessary which is perfomed by plane wave destruction filter to have an accurate amplitude for seismic migration. For verification purpose proposed modelling and diffraction imaging method, we performed modelling the wave propagation in the Sigsbee 2A Model in order to learn wave propagation in a complex velocity field which contains a sedimentary sequence fragmented up by a number of normal and thrust faults (Fig. 7). Moreover, there is a complex salt structure is available in the model that results in illumination problems using the current processing and imaging approach. The model has the features of an absorbing free-surface condition and a weaker than normal water bottom reflection as shown in Fig. 7 (Irons, 2007). This property of the model does not produce the outcome of free surface multiples and less than normal internal multiples. Sigsbee 2A and Sigsbee 2B models are similar, structurally, the only difference being the velocity contrast of the water bottom level.

The same configuration of the survey was designed to model the seismic data for LR and FD, as shown in Figs. 8 and 9 for the accurate evaluation. Dispersion-free seismic was produced using the low-rank approximation for the wave propagation shown in Figs. 8a and 9a. A comparison of the results was achieved by conventional Finite Difference Modelling as shown in Figs. 8b and 9b. The effect of dispersion in the recorded seismic data is minor, as shown by the difference in the simple

velocity model in Fig. 4 as well. This method can be implemented in both the frequency-wavenumber and frequency-space domains. As shown in Figs. 10b and 11b, the use of conventional modelling data for seismic modelling and imaging was unable to illuminate the edges of the subsurface salt body deposit. These problems are very common in current seismic data processing and imaging in the oil and gas industry, but they offer opportunities for researchers to develop new technologies and methods for solving related issues. In this paper, we have used D-Data imaging to solve salt deposit issues.

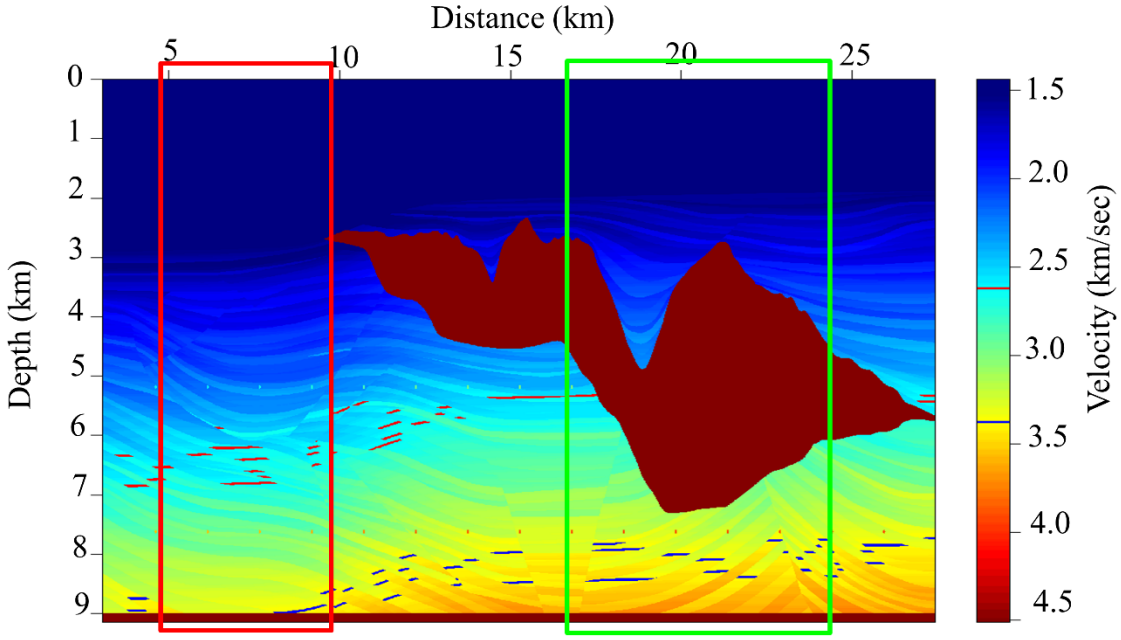

Fig. 7. Sigsbee stratigraphic velocity model with a salt dome of higher velocity between the layered strata. The red and green rectangle shows the extracted model for analysis.

Low-rank wave modelling provides the better preservation of seismic reflection and diffraction at the edges of the salt body. A small part of the seismic section is taken for detailed analysis of wave behavior in a complex structure like Sigsbee and comparison shows with Finite difference modelling (Fig. 8). Fig. 8(a) show with a highlighted red arrow has continuities of hyperbolic behavior on the other hand, in Fig. 8(b) the hyperbola is not sharp, and diffracted energy has a loss with depth.

One of the most common problems in exploration seismic is a vertical resolution for thin-bed identification also related to reflection seismology. Which is the ability to distinguish between two different features with minimum acoustic impedance difference. Improvement in seismic modelling is being able to recover these features as shown in Fig. 9. Fig. 9(a) shows a better delineation of two separate events highlighted with the red arrow and also led to a sharp reflection shown in the red circle. This feature was not recorded in the FD wave modelling as shown in Fig. 9(b), a two-layer bed is not recovered properly. Which is a cause of low vertical seismic resolution.

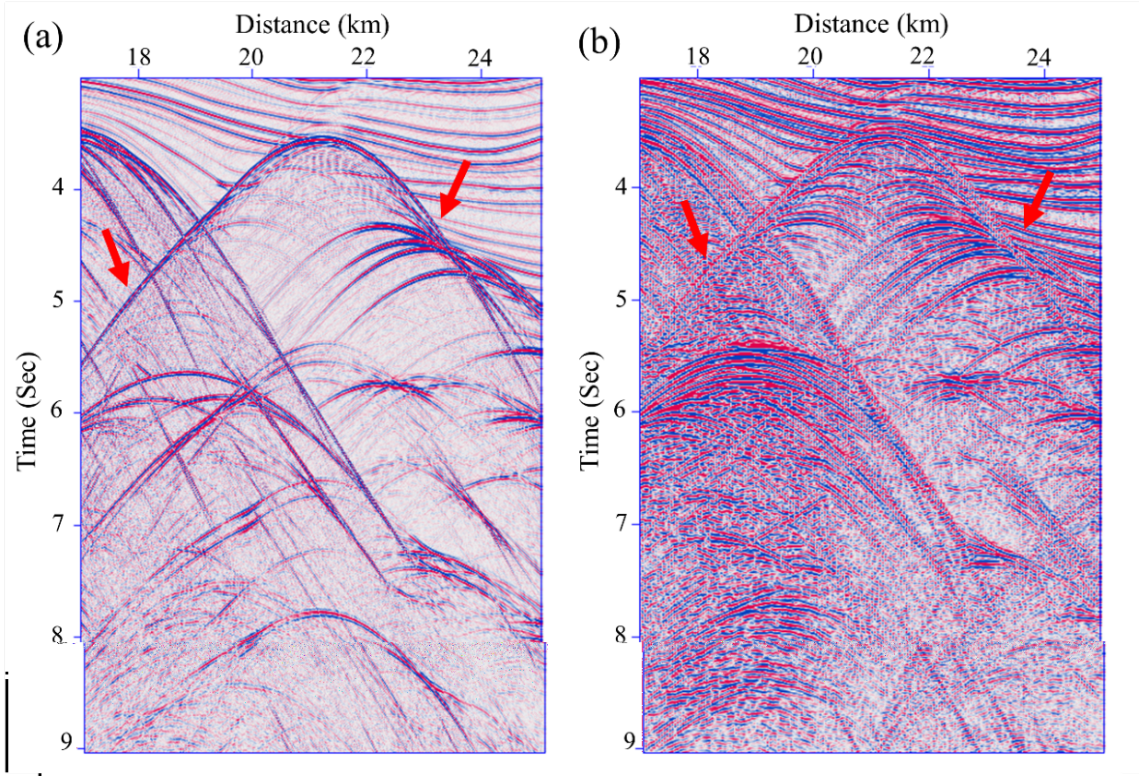

Fig. 8. (a) A cropped seismic section from Sigsbee data using Advance wave modelling, which shows an enhancement of diffraction and preserve the amplitude and phase of the seismic wave, and (b) cropped section using conventional modelling.

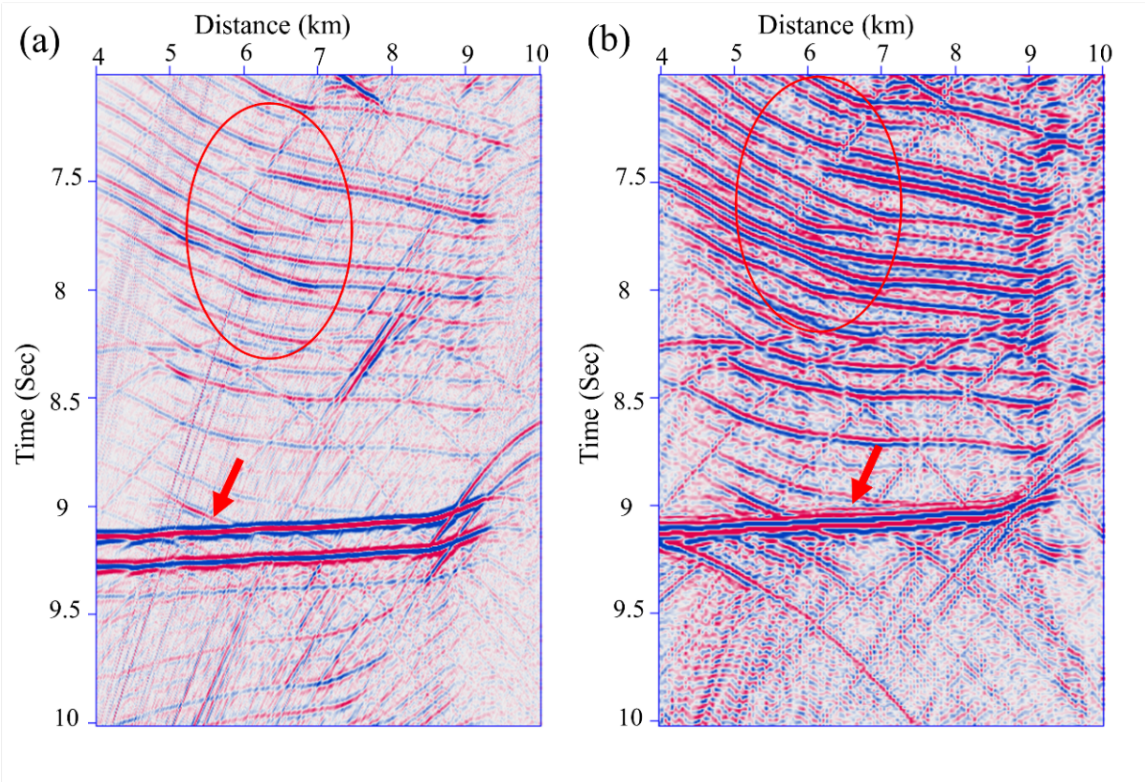

Fig. 9. Improvement in seismic reflection data acquisition (a) reflection data using Advance wave modelling and b) Reflection data using conventional wave modelling.

Fig. 10(a) is the migrated seismic section of the data acquired by LR wave modelling that shows a better reflection data imaging and positioning of layers are accurate as highlighted by the red arrow. Fig. 10(b) is the imaged section using FD wave modelling that has not to recover the horizon properly and shows more than one layer. These poor imaging results would be difficult to interpret as well as the accurate position of the subsurface structure.

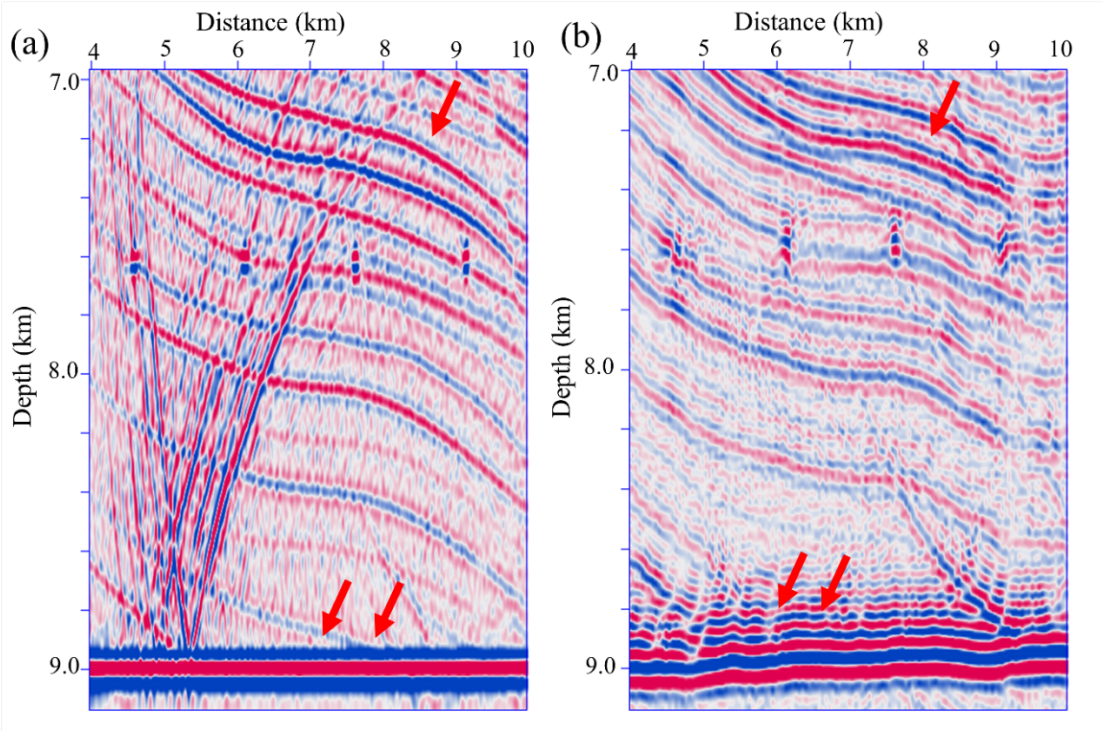

Fig. 10. Final migrated seismic data a) Seismic image with advance wave modelling, show better reflection amplitude and explain the phase correction, and (b) Seismic image using convention modelling, reflection amplitude is dispersed at the reflection point and not recover properly.

Although our main aim is to get a higher resolution image in all over the research, getting the sharp edges of a structure is highly important to define the boundary of the target reservoir. Fig. 11(a) shows the imaged section of the salt body which has recovered all the required objectives, but the FD modelling data has a lack to image the boundaries and edges of the structure shown in Fig. 11(b).

Fig. 12 shows the comparison of the full wave migration of FD (Fig. 12b) and LR wave modelling results (Fig. 12a), which shows an improvement in image quality overall. As it shows the edges of the salt body being illuminated and the reflector below the salt body at a depth of 9 km is imaged by the LR wave modelling data, on the other hand FD wave modelling data is unable to image the reflector.

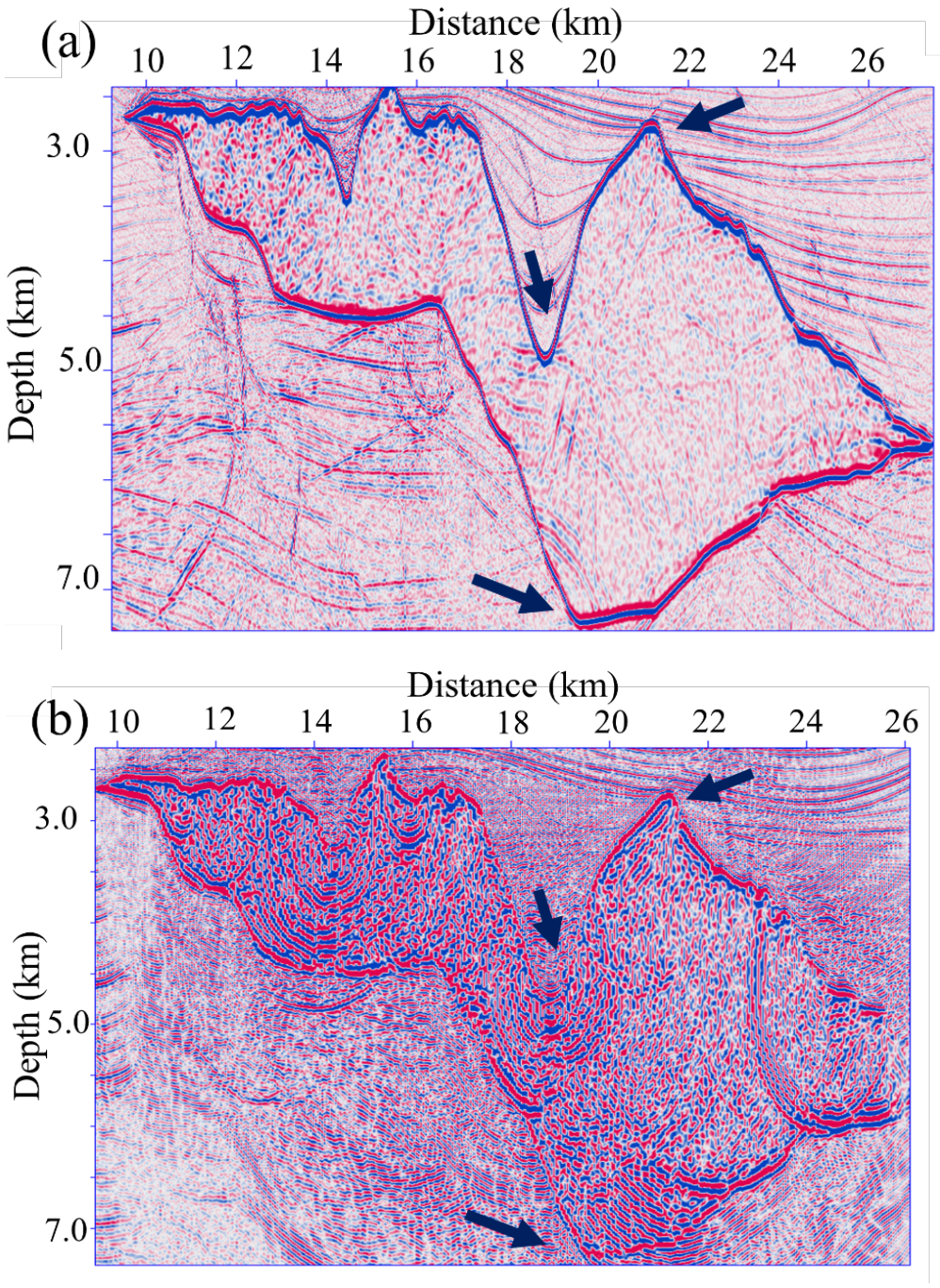

Fig. 11. Final seismic imaging of Salt body structure with edges, (a) seismic image of the salt body using advance wave modelling, shows the significant improvement in imaging (b) conventional modelling, loss of reflection specifically from the edges of the salt body.

The method used for separating the reflection and diffraction data is an improved version of the Claerbout method, which has been used before (Bashir et al., 2017). Fomel contributed to improving the plane-wave destruction filtering technique in 2002 and proved its use on simulated data as well as on real field data.

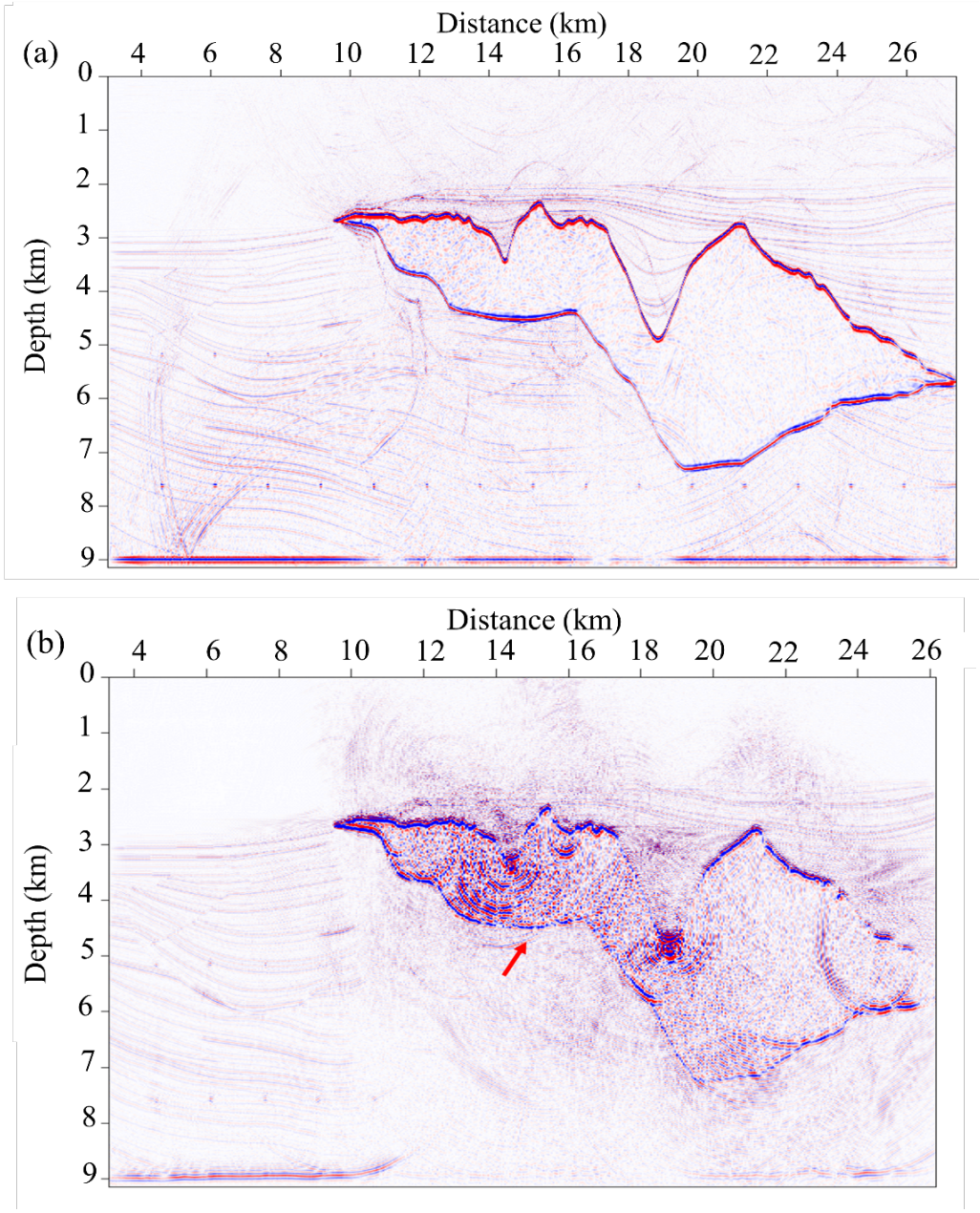

Fig. 12. (a) The outcome of full wave imaging using the proposed low-rank approximation method, and (b) Conventional modelling using the finite difference method and conventional imaging of the data, edges of the salt body are not resolved.

Fig. 13(a) shows the dip component of the model data and recognizes that an exact fortitude of the dipping waves is important because this is an important constraint for PWD filtering, separating reflection and diffraction from full-wave data. In this work, we have separated the seismic diffractions from the reflections using PED filtering (as shown in Fig. 13b) and anxious to image separated diffractions with a accurate velocity model (Fig. 14a); the same velocity model is used for zero-offset reflection migration. Fig. 14(b) is the illustration of frequency spectrums of the migrated data, full wave migration with Split Step Fourier migration is shown in green and diffraction imaging is shown in purple. The frequency spectrum reveals the

preservation of lower frequencies which reflects the deeper events in the data and a higher frequency which reflects the small-scale events and sharp edges of the salt body is improved. Which is a cause of the higher resolution imaging using diffraction data and this long period low frequencies signals are sometime risky for numerous zones of seismic exploration.

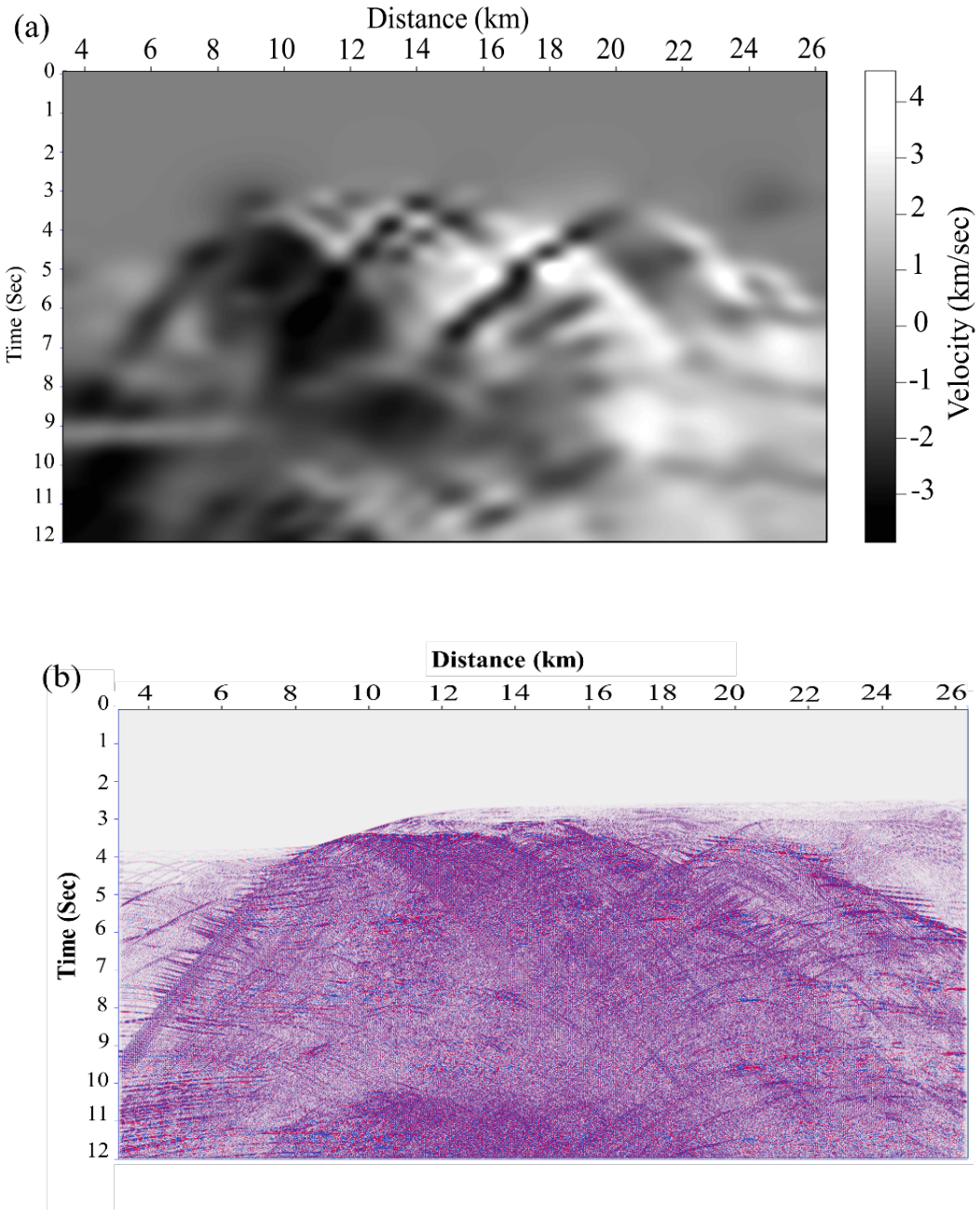

Fig. 13. (a) The calculated dip of the seismic data, using plane wave destruction, (b) separated diffraction after implementation of the plane wave destruction filtering.

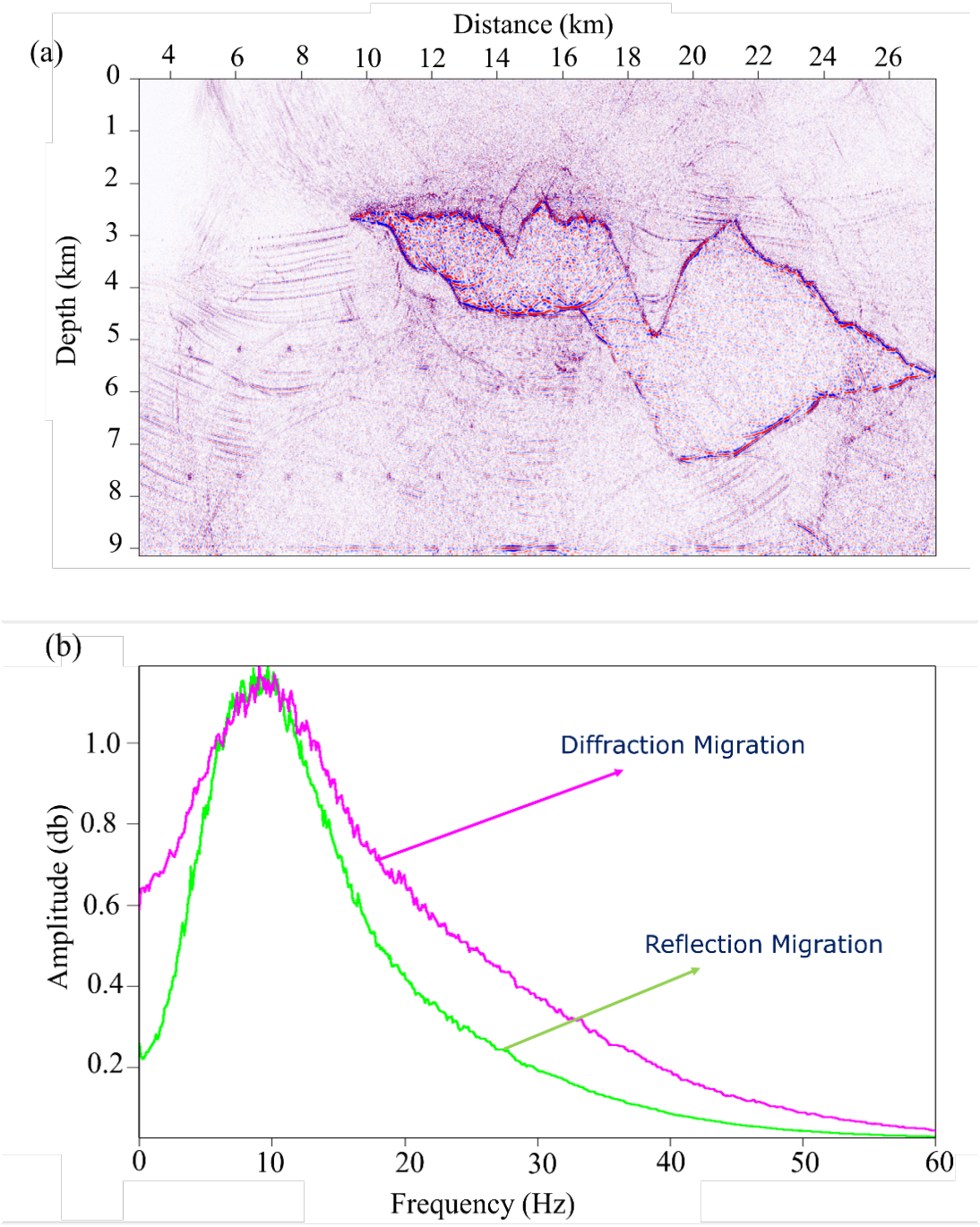

Fig. 14. (a) Diffraction imaging; small-scale events inside the salt bodies are illuminated, and (b) frequency spectrum of full-wave migrated data (green) and diffraction migration (purple). An enhancement of the lower frequency from 0-10 Hz was recovered and high-resolution imaging was recovered for higher frequency data (50 - 60 Hz).

Examples of a complex faulted model: The Marmousi

Secondly, research was extended to a well-known geological model, the Marmousi, which was developed by the Institut Français du Pétrole (IFP) in 1988 (Versteeg, 1994). This model contains 158 horizontally layered horizons and a succession of faulting, that brands it multifaceted,

particularly in the middle. The model is 9.20 kilometres in width and 3 km in depth. Fig. 15a illustrates the Marmousi Model, wherein the challenge is to image the structural reservoir which lies below an anticline. A Ricker wavelet is used to acquire the data using 40 Hz of dominant frequency. The sptial grid size (Δx) was 4 meter and Δz was also 4 meters. Fig. 15b displays the impulse response of the wave propagation at 5 km, to confirm that the propagation effect is real and has a dispersion-free recording system. After carefully defining the acquisition geometry parameters, the zero-offset data set shown in Fig. 15c was achieved.

As our objective was to get a high-resolution image of the 158 layers and associated faulting which can be easily interpreted in the model, this is very challenging for a seismic data processing and imaging geophysicist. Conventional methods are used in (Bashir et al., 2016b) but there are still drawbacks in the final image. A fundamental concept was used innovatively (Fomel, 2002; Fomel et al., 2007a, 2007b; Klokov and Fomel, 2013; Behura, 2009) to produce the high-resolution imaging used in this paper.

Fig. 16a shows the measured dip field of the data using plane-wave destruction filtering for separating diffraction, whilst Fig. 16b estimates the flatness, which is the inverse of the plane-wave destruction filtering for separating reflection data.

The workflow shown in Fig. 6 is an innovative way for high-resolution seismic diffraction imaging. Testing of the workflow is performed on the model data by separating reflection and diffraction. Fig. 17a illustrates the separated diffraction using plane wave destruction filter; diffraction hyperbola can be seen in the red circle, which indicates the 3 major faults as well as a series of diffraction curves on an inclined reflector. Fig. 17b shows the residual reflections, after separating the diffractions from the full wave data.

In conventional migration methods (without diffraction separation and migration), a processing sequence is applied to the raw data without considering diffraction as explained in the workflow. Fig. 18a shows the conventional migrated seismic section which has a low resolution in the shallow parts and the amplitude is not recovered on the targeted area (highlighted with a red circle).

Fig. 18b is the imaged section using the proposed workflow, which contains both reflection migration and diffraction migration separately followed by merging data after migration, shows improvements in resolution, especially for fault amplitude and discontinuities, which were not resolved. For the quantitative accuracy of the results, a frequency spectrum of conventional imaging (red) and diffraction imaging (green) are shown in Fig. 18c. Enhancement of the amplitude recovery from 0 to 10 Hz, improves imaging of the deeper parts as low frequencies travel deeper than high frequencies. Furthermore, low-frequency data produce a higher diffraction response. The amplitude recovery of higher frequency data (between 50 and 60 Hz) is improved for high-resolution imaging in the shallow areas.

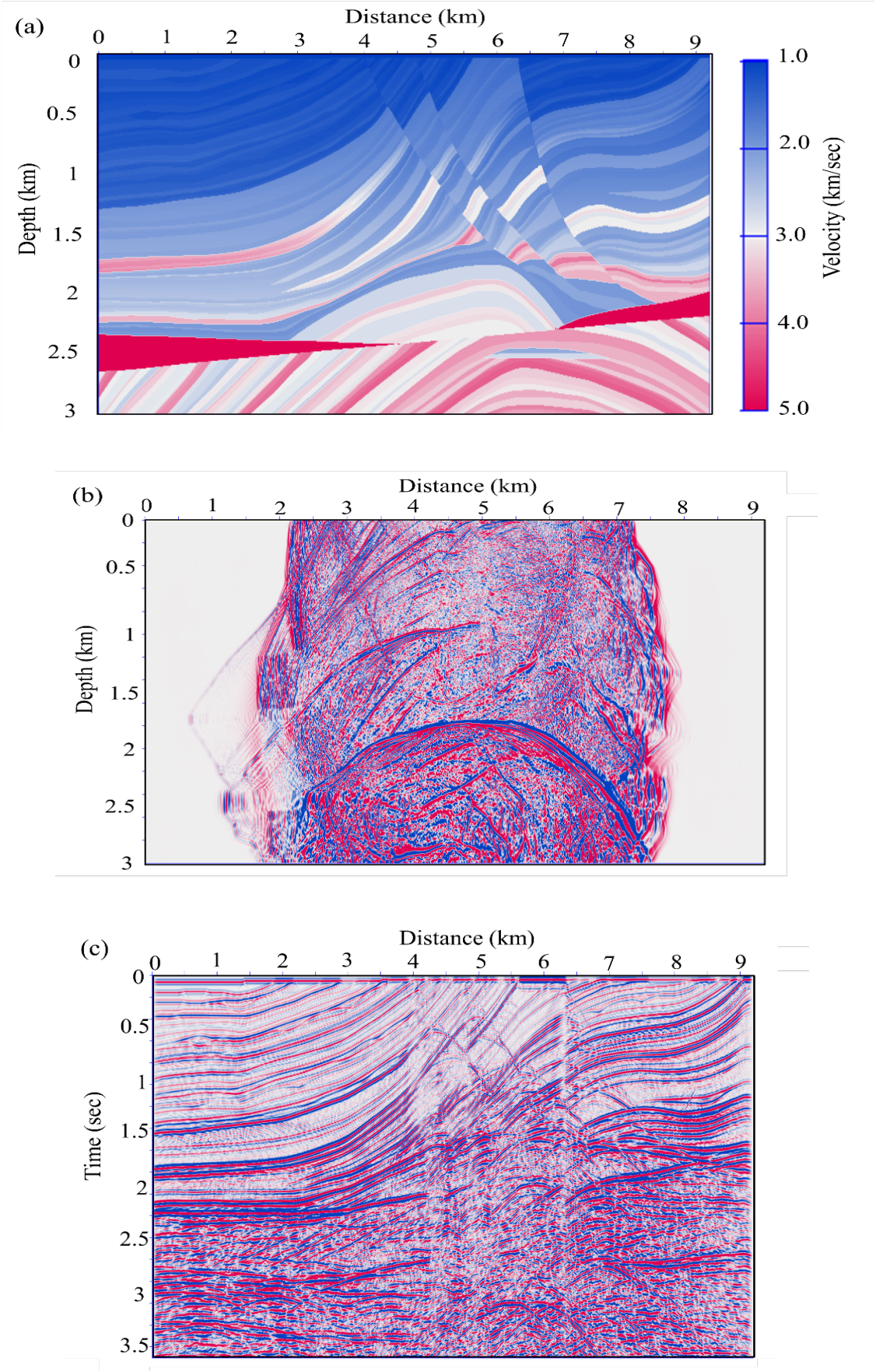

Fig. 15. (a) Marmousi Velocity Model, (b) impulse response of the wave propagation at a 5-kilometer shot point, and (c) zero-offset seismic data.

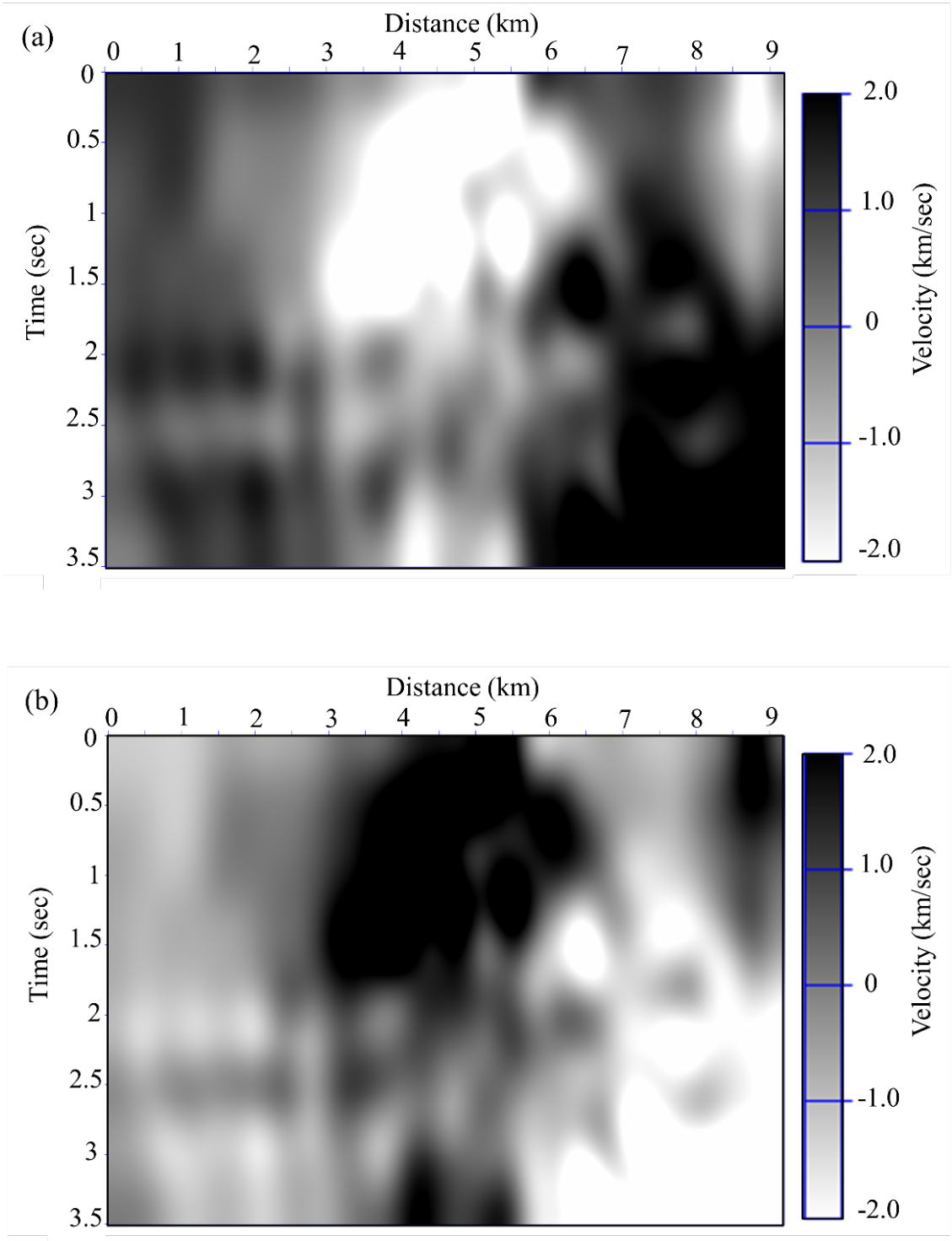

Fig. 16. (a) Estimated slope for the diffraction data separation, and (b) is flatness of the data using inverse plane-wave destruction for reflection data separation.

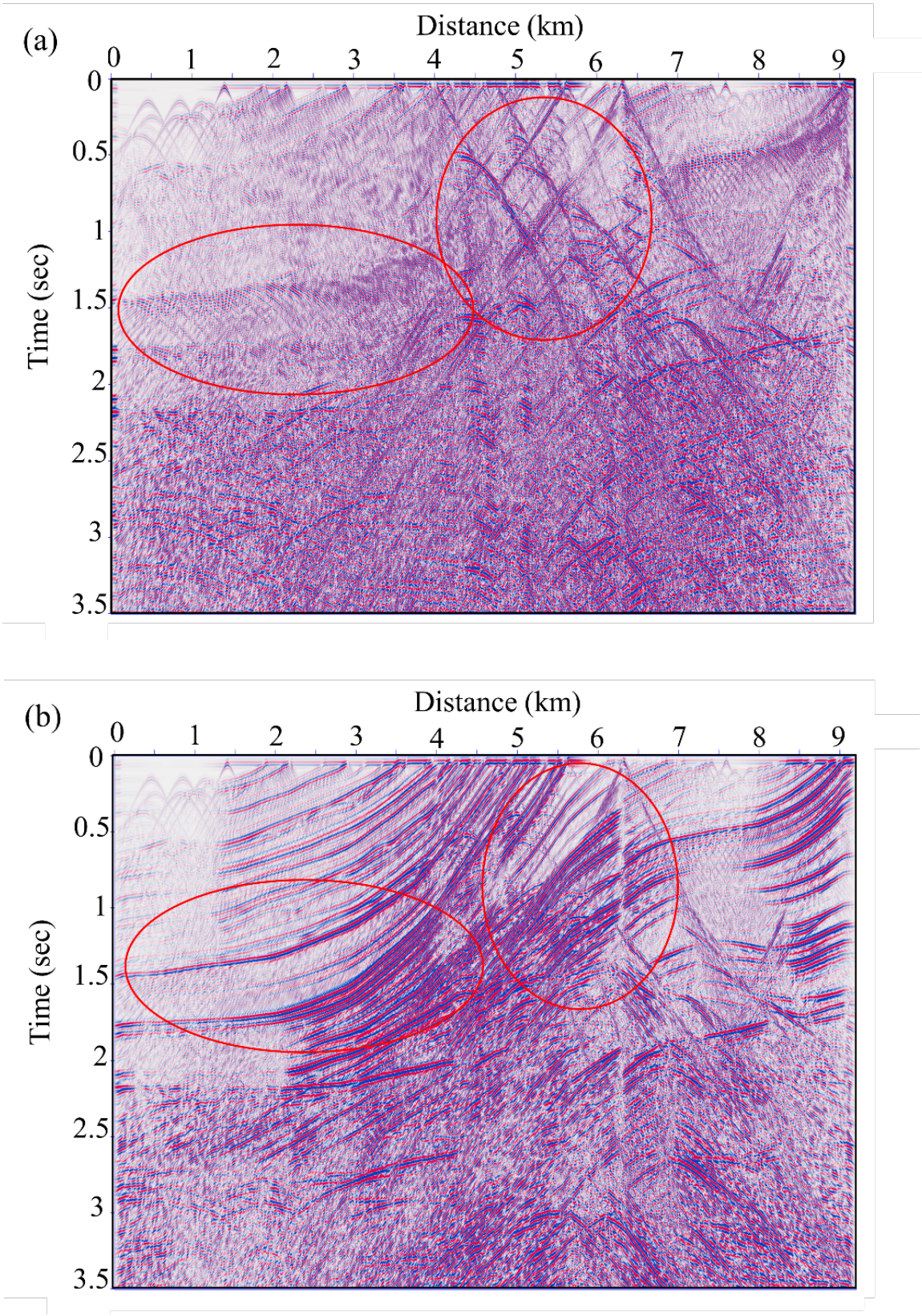

Fig. 17. Application of separation on the seismic response, (a) diffraction only data, and (b) specular reflection data.

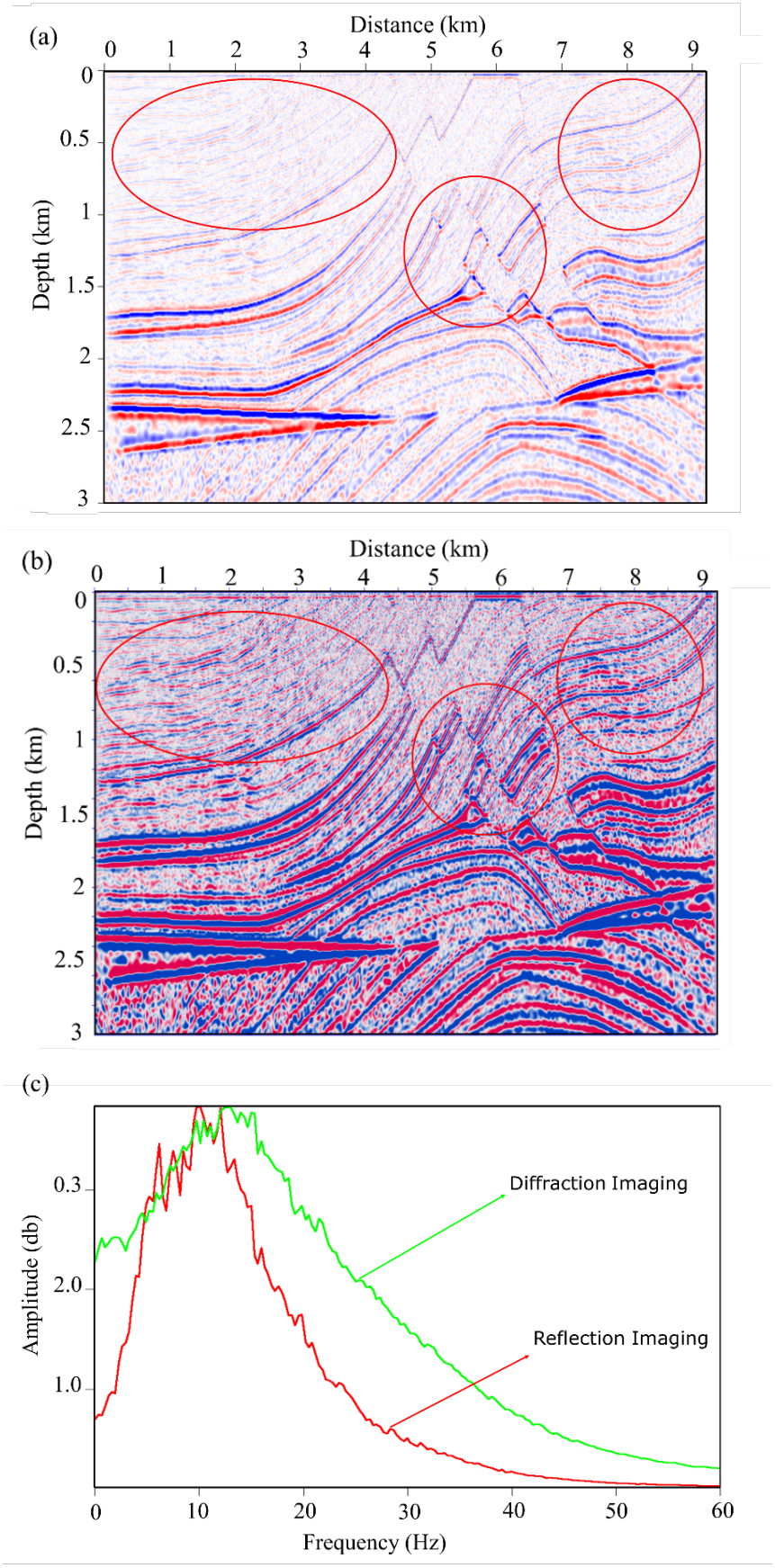

Fig. 18. Appearance of migration results, (a) migrated data using conventional wave propagation modelling, and (b) low rank modelling migration using diffraction data migration, and (c) display data in a frequency spectrum for comparison.

CONCLUSIONS

A low-rank modelling method with a new workflow for imaging is presented to add value to modelling and imaging. Implementation of the proposed workflow has proven for complex structure as Salt deposit (SEG Sigsbee from GOM) and a fractured model data set (EAGE Marmousi). We have presented two different algorithms for the sake of improvements in seismic imaging through wave modelling and diffraction imaging. Comparison of the Finite Difference Method and the low-rank approximation is achieved on the model, which shows that low-rank decomposition for wave approximation is much better and generates data without any dispersion artifacts; the data is best for full-wave imaging with the extended split-step technique.

The second aim of this paper is to incorporate diffractions into seismic imaging, as in the past these diffractions were considered as noise and were suppressed during processing. our research focus remains to preserves diffraction and separate reflection, then migrates these data separately and combines. We found that a combination of these two data sets (full-wave and diffraction imaging) with an accurate velocity model enabled us to produce a high-resolution image. Furthermore, an enhancement of low frequencies data (0 to 10 Hz) for deeper imaging and higher frequencies (50 to 60 Hz) for vertical resolution in the data is achieved. This diffracted image can greatly assist an interpreter when trying to identify structural features, such as the boundaries of salt bodies and reservoirs below the complex, faulted structures on imaged sections.

ACKNOWLEDGMENT

We are thankful to the Universiti Sains Malaysia and the University Teknologi PETRONAS (UTP) for providing the facilities for this research work. In this work, we have used Madagascar as opensource software for performing and developing a workflow for this research work. We would like to thank Sergey Fomel and Luke Decker from the University of Texas at Austin and the Texas Consortium for Computational Seismology, Texas, for their valuable suggestions which helped us to progress our research.

REFERENCES

Bansal, R. and Imhof, M.G., 2005. Diffraction enhancement in prestack seismic data. Geophysics, 70(3): V73-V79. doi.org/10.1190/1.1926577.

Bashir, Y., Ghosh, D.P., Alashloo, S.Y.M. and Sum, C.W., 2016a. Effect of Frequency and Migration Aperture on Seismic Diffraction Imaging. IOP Conf. Series: Earth and Environmental Science, Vol. 30. doi.org/10.1088/1755-1315/30/1/012001.

Bashir, Y., Ghosh, D.P., Alashloo, S.Y.M. and Sum, C.W., 2016b. Enhancement in Seismic Imaging Using Diffraction Studies and Hybrid Traveltime Technique for PSDM. IOP Conf. Series: Earth and Environmental Science. Vol. 38. doi.org/10.1088/1755-1315/38/1/012002.

Bashir, Y., Ghosh, D. and Sum, C.W., 2017. Preservation of seismic diffraction to enhance the resolution of seismic data. Expanded Abstr., 87th Ann. Internat. SEG Mtg., Houston: 1038-1043.

Bashir, Y., Ghosh, D.P. and Sum, C.W., 2018. Influence of seismic diffraction for high-resolution imaging: applications in offshore Malaysia. Acta Geophys., 66: 305-316. doi.org/10.1007/s11600-018-0149-7.

Bashir, Y., Latif, A.H.A., Rezaei, S., Mahgoub, M., Alashloo, S.Y.M., Hermana, M., Ghosh, D.P. and Sum, C.W., 2019. Seismic diffraction imaging in laterally varying velocity media for frequency bandwidth expansion-application in carbonate field Sarawak, Malaysia. Internat. Petrol. Conf., Soc. Petrol. Engin., Abu Dhabi.

Bashir, Y., Alashloo, S.Y.M., Latiff, A.H.A., Mahgoub, M., Hermana, M. and Ghosh, D., 2020. Seismic wave features in anisotropic modeling and effects in imaging complex subsurface structure. Internat. Petrol. Technol. Conf., Dhahran.

Behura, J., 2009. Estimation and Analysis of Attenuation Anisotropy. Vol. 71, Citeseer.

Behura, J. and Tsvankin, I., 2009. Role of the inhomogeneity angle in anisotropic attenuation analysis. Geophysics, 74(5): WB177-WB191.

Berryhill, J.R., 1977. Diffraction response for nonzero separation of source and receiver. Geophysics, 42: 1158-1176. doi.org/doi:10.1190/1.1440781.

Coimbra, T.A., Faccipieri, J.H., Speglich, J.H., Gelius, L.-J. and Tygel, M., 2018. Enhancement of diffractions in prestack domain by means of a finite-offset double-square-root traveltime. Geophysics, 84(1): V81-V96.

Dablain, M.A., 1986. The application of high-order differencing to the scalar wave equation. Geophysics, 51: 54-66.

Etgen, J.T. and Brandsberg-Dahl, S., 2009. The pseudo-analytical method: application of pseudo-Laplacians to acoustic and acoustic anisotropic wave propagation. Expanded Abstr., 79th Ann. Internat. SEG Mtg., Houston: 2552-2556.

Fomel, S., 2002. Applications of plane-wave destruction filters. Geophysics, 67: 1946-1960.

Fomel, S., Landa, E. and Taner, M.T., 2007a. Diffraction imaging for fracture detection. Workshop Package , 69th EAGE Conf., London.

Fomel, S., Landa, E. and Taner, M.T., 2007b. Poststack velocity analysis by separation and imaging of seismic diffractions. Geophysics, 72(6): U89-U94.

Fomel, S., Ying, L. and Song, X., 2013. Seismic wave extrapolation using lowrank symbol approximation. Geophys. Prosp., 61: 526-536.

Hilterman, F.J., 1975. Amplitudes of seismic waves; a quick look. Geophysics, 40: 745-762. doi.org/10.1190/1.1440565.

Hilterman, F.J., 1970. Three-dimensional seismic modeling. Geophysics, 35: 1020-1037. doi.org/doi:10.1190/1.1440140.

Holberg, O., 1988. Towards optimum one-way wave propagation, 1. Geophys. Prosp., 36: 99-114.

Holloway, N.H., 1981. The North Palawan Block, Philippines: Its relation to the Asian mainland and its role in the evolution of the South China Sea. AAPG Bull., 66: 1355-1383.

Kindelan, M., Kamel, A. and Sguazzero, P., 1990. On the construction and efficiency of staggered numerical differentiators for the wave equation. Geophysics 55: 107-110.

Klokov, A. and Fomel S., 2013. Seismic diffraction imaging, one migration dip at a time. Expanded Abstr., 83rd Ann. Internat. SEG Mtg., Houston: 3697-3702.

Landa, E. and Keydar, S., 1998. Seismic monitoring of diffraction images for detection of local heterogeneities. Geophysics, 63: 1093-1100.

Liu, Y. and Sen, M.K., 2009. A new time–space domain high-order finite-difference method for the acoustic wave equation. J. Comput. Phys., 228: 8779-8806.

Liu, Y. and Sen, M.K., 2011. Finite-difference modeling with adaptive variable-length spatial operators. Geophysics, 76(4): T79-T89.

Mousa, W.A., van der Baan, M., Boussakta, S. and McLernon. D.C., 2009. Designing stable extrapolators for explicit depth extrapolation of 2D and 3D wavefields using projections onto convex sets. Geophysics, 74(2): S33-S45.

Neal, J. and Krohn, C., 2012. Higher resolution subsurface imaging. J. Petrol. Technol., 64(3): 44-53.

Song, X., Fomel, S. and Ying, L., 2013. Lowrank finite-differences and lowrank Fourier finite-differences for seismic wave extrapolation in the acoustic approximation. Geophys. J. Internat., 193: 960-969.

Soubaras, R., 1996. Explicit 3-D migration using equiripple polynomial expansion and Laplacian synthesis. Geophysics, 61: 1386-93.

Takeuchi, N. and Geller, R.J., 2000. Optimally accurate second order time-domain finite difference scheme for computing synthetic seismograms in 2-D and 3-D media. Phys. Earth Planet. Inter., 119: 99-131.

Taner, M.T., Fomel, S. and Landa, E., 2006. Separation and imaging of seismic diffractions using plane-wave decomposition. Expanded Abstr., 76th Ann. Internat. SEG Mtg., New Orleans: 2401-2405.

Versteeg, R., 1994. The Marmousi Experience; Velocity model determination on a synthetic complex data set. The Leading Edge, 13: 927-936. http://tle.geoscienceworld.org/content/13/9/927.short.

Wards, B.D., Margrave, G.F. and Lamoureux, M.P., 2008. Phase-shift time-stepping for reverse-time migration. Expanded Abstr., 78th Ann. Internat. SEG Mtg., Las Vegas: 2262-2266.